A Kinetic Mechanism for Cleavage of Precursor tRNA^{Asp} Catalyzed by the RNA Component of *Bacillus subtilis* Ribonuclease P†

Jane A. Beebe and Carol A. Fierke*

Department of Biochemistry, Box 3711, Duke University Medical Center, Durham, North Carolina 27710

Received April 14, 1994; Revised Manuscript Received June 22, 1994®

ABSTRACT: A kinetic mechanism is presented for the cleavage of *Bacillus subtilis* precursor tRNA^{Asp} catalyzed by the RNA component of *B. subtilis* ribonuclease P (RNase P) under optimal conditions (50 mM Tris Cl (pH 8.0), 100 mM $MgCl_2$, and 800 mM NH_4Cl, 37 °C). This kinetic mechanism was derived from measuring pre-steady-state, steady-state, single-turnover, and binding kinetics using a combination of quench-flow, gel filtration, and gel shift techniques. A minimal kinetic description involves the following: (1) binding of pre-tRNA^{Asp} to RNase P RNA rapidly (6.3×10^6 M^{-1} s^{-1}), but slower than the diffusion-controlled limit; (2) cleavage of the phosphodiester bond with a rate constant of 6 s^{-1}; (3) dissociation of products in a kinetically preferred pathway, with the 5′ RNA fragment dissociating first ($\geq$0.2 s^{-1}) followed by rate-limiting tRNA dissociation (0.02 s^{-1}); and (4) formation of a second conformer of RNase P RNA during the catalytic cycle that is less stable and binds pre-tRNA^{Asp} significantly more slowly (7×10^4 M^{-1} s^{-1}). This scheme involves the isolation of individual steps in the reaction sequence, is consistent with steady-state data, and pinpoints the rate-determining step under a variety of conditions. This kinetic mechanism will facilitate a more accurate definition of the role of metals, pH, and the protein component in each step of the reaction and provide an essential background for understanding the influence of structural changes on the catalytic activity.

Ribonuclease P (RNase P[1]), a ribonucleoprotein complex, catalyzes the essential 5′ maturation of precursor tRNA (pre-tRNA) [see reviews: Altman (1989) and Pace and Smith (1990)]. In diverse organisms, this enzyme is composed of two subunits: an RNA moiety (about 400 nucleotides) and a protein (about 120 amino acids) moiety. While both are essential for *in vivo* activity, the RNA component from bacterial RNase P is sufficient to catalyze the specific cleavage of pre-tRNA *in vitro* in the presence of high salt, demonstrating that the RNA component is catalytic. Other RNAs that can specifically cleave nucleic acids are known [see review: Pyle (1993)]; however, RNase P is the only RNA-containing nuclease that truly behaves as an enzyme *in vivo* since it catalyzes multiple turnovers and is unchanged during catalysis. Moreover, this enzyme plays an essential physiological role in the formation of functional tRNA molecules (Abelson, 1979; Robertson et al., 1972). Investigation of the chemical mechanism and structure–function properties of RNase P should lead to a greater understanding of the fundamentals of ribozyme function and aid in the design of more efficient ribozymes directed toward gene inactivation.

RNase P catalyzes the cleavage of P–3′O bonds to produce 5′-phosphate and 3′-hydroxyl end groups at a specific site on pre-tRNA, but the mechanism of this reaction is still under investigation. Catalysis of pre-tRNA cleavage by the RNA subunit of RNase P, as assayed by steady-state turnover, is pH independent, has a metal ion dependence (Mg^{2+}, Mn^{2+}, or Ca^{2+}), does not result in the accumulation of any covalent intermediates, and is increased by the addition of high salt (Altman, 1989; Pace & Smith, 1990). However, mechanistic studies measuring the steady-state hydrolysis of pre-tRNA have been hampered since the rate-limiting step is likely tRNA dissociation, not chemical cleavage (Reich et al., 1988; Tallsjö & Kirsebom, 1993). This difficulty has been addressed by decreasing the hydrolytic rate constant either by substitution of a deoxynucleotide at the cleavage site or by lowering the reaction pH (Smith & Pace, 1993). These experiments indicate that RNase P-catalyzed cleavage is pH dependent and requires several magnesium ions, suggesting that hydroxide or metal-bound hydroxide might function as a nucleophile in the cleavage reaction.

As a prerequisite for further mechanistic studies of RNase P, we have elucidated a complete kinetic sequence for the cleavage of pre-tRNA^{Asp} catalyzed by the RNA component of RNase P, using a combination of quench-flow, gel filtration, and gel shift techniques to measure pre-steady-state, single-turnover, steady-state, and binding kinetics. This work constitutes the first complete kinetic scheme for any variety of RNase P and the first reported use of a chemical quench-flow instrument in the study of catalytic RNAs. A minimal kinetic description is shown in Figure 1 and includes the following: (1) rapid, essentially irreversible binding of pre-tRNA; (2) essentially irreversible cleavage of pre-tRNA; (3) rapid dissociation of the 5′ RNA fragment (5′P); (4) slow dissociation of tRNA; and (5) slow equilibration between two enzyme forms. In the future, this approach will be used to assay the effects of pH, mono- and divalent cation concentrations, substrate and enzyme structures, and the protein component on each of these steps with a physiological substrate. This will lead to a greater understanding of the catalytic

† Supported by National Institutes of Health Grant GM40602. C.A.F. received a David and Lucile Packard Foundation Fellowship in Science and Engineering and an American Heart Association Established Investigator Award.

* Author to whom correspondence should be addressed. Telephone: (919) 684-2557. FAX: (919) 684-8885.

® Abstract published in *Advance ACS Abstracts,* August 1, 1994.

[1] Abbreviations: RNase P, ribonuclease P; Tris, tris(hydroxymethyl)-aminomethane; EDTA, (ethylenedinitrilo)tetraacetic acid; TE buffer, 10 mM Tris (pH 8) and 1 mM EDTA; GTP, guanosine triphosphate; NP40, nonidet P40 or α-(ethylphenyl)poly(ethylene glycol); SDS, sodium dodecyl sulfate; buffer 1, 100 mM $MgCl_2$, 800 mM NH_4Cl, 50 mM Tris-HCl (pH 8.0), 0.05% NP40, and 0.1% SDS; pre-tRNA, precursor tRNA; 5′P, 5′ precursor tRNA fragment; E, RNA component of RNase P; cpm, counts per minute.

0006-2960/94/0433-10294$04.50/0

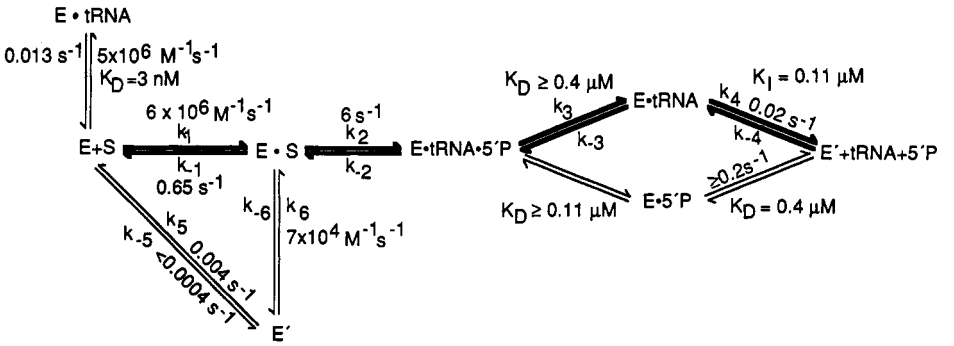

FIGURE 1: Kinetic mechanism for cleavage of pre-tRNA^{Asp} catalyzed by the RNA component of *B. subtilis* RNase P at 37 °C in 100 mM $MgCl_2$, 800 mM NH_4Cl, 50 mM Tris (pH 8), 0.05% NP40, and 0.1% SDS: E, RNA component of RNase P; E′, additional conformer of the RNA component of RNase P; S, pre-tRNA^{Asp}; 5′P, 5′ precursor fragment; tRNA, mature tRNA^{Asp}.

mechanism of RNase P by providing more detailed mechanistic information than that gained by solely measuring steady-state kinetic parameters. Furthermore, this kinetic and thermodynamic analysis of RNase P may provide insight into the mechanisms of other ribozymes and facilitate comparison to the mechanisms of rate acceleration for protein catalysts as well.

MATERIALS AND METHODS

RNA Preparation and Quantitation. Plasmids pDW25 and pDW152 were generous gifts from the laboratory of Dr. Norman Pace (Indiana University). Plasmid pDW25 was linearized with the restriction enzyme *Dra*I followed by *in vitro* transcription (Milligan & Uhlenbeck, 1989; Reich et al., 1988) to produce the *Bacillus subtilis* RNase P RNA component. Plasmid pDW152 was cut with *Bst*NI followed by *in vitro* transcription to yield a precursor of *B. subtilis* tRNA^{Asp} with a mature 3′ end. T7 RNA polymerase was purified from an overexpressing strain provided by W. Studier (Davanloo et al., 1984). Pre-tRNA^{Asp} was labeled by including [α-^{32}P]GTP in the *in vitro* transcription reaction. Products were separated by denaturing polyacrylamide gel electrophoresis (5–8% polyacrylamide/8 M urea) and identified by UV shadowing (Sambrook et al., 1989). The RNA was isolated by soaking the bands in 10 mM Tris-HCl (pH 8.0), 1 mM EDTA (TE buffer), and 0.1% sodium dodecyl sulfate (SDS) and then purified by ethanol precipitation followed by gel filtration chromatography (Sephadex G-50 for RNase P RNA and G-25 for pre-tRNA^{Asp}). To produce either mature tRNA^{Asp} or 5′ fragment (5′P), pre-tRNA^{Asp} was cleaved with RNase P RNA, and products were separated and purified as described. tRNA type XX from *Escherichia coli* strain W (Sigma) was dissolved in TE (pH 8), extracted once with phenol/chloroform (1:1) and twice with chloroform, and then precipitated with ethanol before use.

Extinction coefficients for the native RNAs were determined as follows. The RNA samples were hydrolyzed to ribonucleotides (0.1 M NaOH for 3 h, 25 °C), the absorbance at 260 nm (pH 11) was determined, and then the RNA concentration was calculated using the extinction coefficients for each individual ribonucleotide (Zaug et al., 1988; Dawson et al., 1986). The extinction coefficient of the intact RNA was then calculated from its absorbance at 260 nM and the concentration determined above: $\epsilon_{260} = 3.94 \times 10^6$ M^{-1} cm^{-1} for RNase P RNA, 9.89×10^5 M^{-1} cm^{-1} for pre-tRNA^{Asp}, 6.43×10^5 M^{-1} cm^{-1} for tRNA^{Asp}, and 3.09×10^5 M^{-1} cm^{-1} for 5′P.

Steady-State Experiments. Experiments were performed under conditions of excess substrate ([S]/[E] ≥ 5) in buffer 1, which contains the following: 100 mM $MgCl_2$, 800 mM NH_4Cl, 50 mM Tris-HCl (pH 8.0), 0.05% nonidet P40 (NP40), and 0.1% SDS. These conditions are optimal for the steady-state cleavage of pre-tRNA^{Asp} catalyzed by RNase P RNA (Reich et al., 1988). Each type of RNA was resuspended in TE, heated to 95 °C for 3 min, mixed with an equal volume of 2× buffer 1, and allowed to preincubate for 15 min at 37 °C. The observed steady-state rate is not dependent on the length of time of preincubation (15–60 min). Reactions were initiated by the addition of enzyme, incubated at 37 °C, and quenched by the addition of an equal volume of 10 M urea, 200 mM EDTA (pH 8.0), 0.1% bromophenol blue, and 0.1% xylene cyanol. Additionally, reactions were quenched with a 2.5-fold volume of ethanol or an equal volume of 10% trichloroacetic acid. Identical results were obtained with all three quenches (data not shown). Reaction products were separated on an 8% polyacrylamide gel containing 8 M urea and visualized by autoradiography and quantitated by scintillation counting of excised bands or visualized and quantitated using a PhosphorImager from Molecular Dynamics. The average error in reaction rates for these experiments was 20%, as determined from the standard deviation of multiple (>3) data points collected under identical conditions.

Pre-Steady-State and Single-Turnover Experiments. For experiments in which short incubation times (0.005–10 s) were required, a model RQF-3 quench-flow apparatus from Kin-Tek instruments was used. Detailed information on the use of this quench-flow instrument, including a diagram, has been reported (Johnson, 1986, 1992). This chemical quench-flow apparatus allows the mixing of two reactants for a specified time interval, followed by mixing with a quenching agent to stop the reaction. The instrument was flushed with autoclaved water before use and between reactions. The temperatures of the sample and reaction loops were maintained at 37 °C by a circulating water bath. RNase P RNA (0.06–19 μM) and pre-tRNA^{Asp} (0.012–0.1 μM), pretreated as described above, were loaded into two separate 1-mL syringes used to fill the 40-μL sample loops. The drive syringes were then pushed at a constant velocity to mix the enzyme and substrate in a 1:1 ratio, and the reaction proceeds as the mixture flows through a reaction loop of defined length. The reaction was terminated by mixing it with 2.1 vol of 90 mM EDTA in a second mixer (final concentrations, 61 mM EDTA and 32 mM $MgCl_2$). This solution then flowed through the exit line into a waiting Eppendorf tube containing urea and dyes (bromophenol blue and xylene cyanol) to final concentrations of 4 M and 0.05%, respectively. The time of the reaction (5 ms to 10 s) was determined by both the volume of the reaction loop between the two points of mixing and the rate of flow. Each time point used approximately 40 μL of each reactant solution. The reaction products were separated and quantitated as described for the steady-state experiments. Identical results were obtained with a 5% trichloroacetic acid quench.

For tRNA trap experiments (Rose, 1980), RNase P RNA (0.01–19 μM) and pre-tRNA^{Asp} (0.012–0.024 μM) in buffer 1 at 37 °C were mixed and incubated for 0.005–5 s in the quench-flow instrument, as described above, and quenched by mixing with 2.1 vol of 58 μM tRNA type XX (final concentration, 39.3 μM). Then the reaction was incubated for 15–20 s (tRNA trap step) and stopped by the addition of an equal volume of 10 M urea/300 mM EDTA. The amount of pre-tRNA cleavage is independent of the incubation time with tRNA over a range of 10–440 s (data not shown). An average of 10% error in the observed rate constant was obtained for experiments performed using the quench-flow apparatus.

Gel Shift Assays. The RNA component of RNase P (0–30 nM) and ^{32}P-labeled mature tRNA^{Asp} (0.1 nM) were prepared separately, as described, and then incubated together for 1 h at 37 °C. This length of time was sufficient for the reaction to reach equilibrium, as determined by varying the length of preincubation (30–120 min) or by calculating k_{obs} from the association and dissociation rate constants. A 10× loading buffer containing 40% glycerol and 0.5% xylene cyanol was added, and the sample was loaded onto a 10% polyacrylamide gel (14 cm × 17 cm × 1 mm) running at 50 V (constant voltage, current ≈ 350 mA). Electrophoresis was carried out for about 6 h until the xylene cyanol band migrated approximately $^3/_4$ in. (Hardt et al., 1993; Pyle et al., 1990), with the gel temperature maintained by circulating 37 °C water through the electrophoresis cell. Both the gel and running buffer contained the following: 50 mM Tris–acetate (pH 8.0), 100 mM magnesium acetate, 800 mM NH_4Cl, and 0.1 mM EDTA. This high concentration of salt was necessary to obtain tight binding of tRNA to RNase P RNA. Bands were fairly sharp, as shown in Figure 7. Any radioactivity migrating slower than tRNA^{Asp} was treated as bound material.

Centrifuge Columns. To measure the dissociation constant, RNase P RNA (0–30 nM) and ^{32}P-labeled mature tRNA^{Asp} (0.1 nM) were prepared as described and then incubated together for 1 h at 37 °C. Gel filtration centrifuge columns (Penefsky, 1979; Sambrook et al., 1989) were prepared by centrifuging 600 μL of Sephadex G-75 resin suspended in buffer 1 in Spin-X centrifuge filter units (Costar) at 4000 rpm for 1 min. Then, 20 μL of the sample containing ^{32}P-labeled tRNA^{Asp} and RNase P RNA was added, and the column was spun again at 4000 rpm for 1 min. The gel matrix was separated from the eluate, and the ^{32}P-labeled tRNA contained in each was quantitated by scintillation counting. About 25% of the radioactivity from ^{32}P-labeled tRNA^{Asp} was measured in the eluate in the absence of RNase P RNA ($cpm_{background}$), and about 90% was measured at high [RNase P RNA] ($cpm_{end\ point}$). The fraction of tRNA bound ([E·tRNA]/[$tRNA_{tot}$]) was calculated as (cpm_{eluate} − $cpm_{background}$)/($cpm_{end\ point}$ − $cpm_{background}$), where cpm is the radioactivity in counts per minute. Using this method, high molecular weight species are eluted from the column, while small molecules remain sequestered at the top of the column (Penefesky, 1979). Small molecules may be eluted by the addition of 150 μL of buffer 1 and centrifugation.

To measure k_{off}, ^{32}P-labeled tRNA^{Asp} (0.1 nM) and RNase P RNA (30 nM) were incubated together for 1 h, then unlabeled tRNA^{Asp} (100 nM) was added so that the final concentration of tRNA was 1000-fold greater than that of ^{32}P-labeled tRNA^{Asp}. The RNA was loaded onto a gel filtration centifuge column at specific time intervals after dilution, and the counts in the eluate were quantitated by scintillation counting. To measure k_{obs} for the formation of the E·tRNA^{Asp} complex, mature ^{32}P-labeled tRNA^{Asp} (0.5 nM) was mixed with RNase P RNA (2.7–8.1 nM) and loaded onto the column at specific time intervals, and the counts in the eluate were quantitated with scintillation counting. An average of 12% error in the fraction of tRNA bound to RNase P RNA was observed for experiments performed using centrifuge columns.

Data Analysis. Data were fit with the KaleidaGraph (Synergy Software) curve-fitting program using the equations described here (Fierke & Hammes, 1994; Johnson, 1992), and the reported errors are the asymptotic standard errors. For single-turnover experiments, the time course for the appearance of products (as measured by radioactivity in counts per minute (cpm)) was fit to a mechanism of either a single first-order reaction (eq 1) or two consecutive first-order reactions (eq 2):

$$[P] = [P]_\infty(1 - e^{-k_{obs}t}) \quad (1)$$

$$[P] = [\text{pre-tRNA}]_0\left[1 + \frac{1}{k_1 - k_2}(k_2e^{-k_1t} - k_1e^{-k_2t})\right] \quad (2)$$

where t is time and [P] is the fraction of pre-tRNA cleaved [=(cpm_{tRNA} + $cpm_{5'P}$)/($cpm_{pre\text{-}tRNA}$ + cpm_{tRNA} + $cpm_{5'P}$)]. For pre-steady-state experiments, data are fit to eq 3, in which the appearance of [P] is described by the sum of a line representing steady-state turnover and a single first-order exponential, where A and k_{burst} indicate the amplitude and observed rate constant of the burst, respectively.

$$[P] = \frac{k_{cat}[E]_0[S]_0t}{K_M + [S]_0} + A[E]_0[1 - e^{-k_{burst}t}] \quad (3)$$

For the measurement of k_{off} for tRNA, the disappearance of radioactivity (cpm) in the eluate was observed, and these data were analyzed using eq 4:

$$(cpm)_{eluate} = (cpm)_{total}\,(e^{-k_{off}t}) \quad (4)$$

Dissociation constants were determined by fitting the data to eq 5:

$$[tRNA]_{bound}/[tRNA]_{total} = 1/(1 + K_D/[E]_{total}) \quad (5)$$

Steady-state kinetic parameters and inhibition constants were determined from eqs 6 and 7, respectively:

$$\text{initial velocity} = k_{cat}[E][S]/(K_M + [S]) \quad (6)$$

$$\text{initial velocity} = k_{cat}[E][S]/(K_M(1 + [I]/K_I) + [S]) \quad (7)$$

RESULTS

Pre-Steady-State Burst. Reich et al. (1988) observed two phases in a time course for the cleavage of pre-tRNA^{Asp} catalyzed by the RNA component of *B. subtilis* RNase P (50 mM Tris-HCl (pH 8.0), 0.5% NP40, 2 M NH_4Cl, and 100 mM $MgCl_2$): an initial "burst" of tRNA at short times, followed by a linear increase in the concentration of tRNA. These data are consistent with any two-step kinetic mechanism in which binding and hydrolysis occur in the first step followed by regeneration of the active catalyst in a rate-limiting second step (Fierke & Hammes, 1994; Johnson, 1992). We repeated these experiments at a higher ratio (5:1) of substrate to enzyme using a quench-flow instrument to measure both the rate constant and amplitude of the burst. A time course for the hydrolysis of pre-tRNA^{Asp} under conditions of excess substrate (Figure 2) clearly illustrates a pre-steady-state burst with an amplitude dependent on the concentration of RNase P RNA. Fitting of the time course at 20 nM RNase P RNA with eq 3 allows calculation of the amplitude and the observed rate

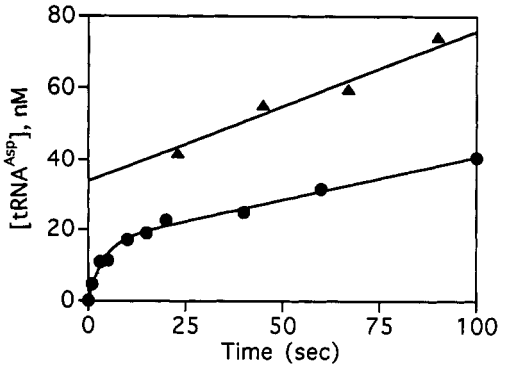

FIGURE 2: Time course for hydrolysis of pre-tRNA^{Asp} ([pre-tRNA]/[E] = 5) catalyzed by either 20 (●) or 40 nM (▲) RNA component of RNase P. Data were obtained at 20 nM RNase P RNA with the use of a KinTek RQF-3 rapid quench instrument, and data at 40 nM RNase P RNA were obtained by quenching the reaction manually. Data measured at 40 nM RNase P RNA were fit to an equation for a straight line, slope/[E] = 0.011 s^{-1}; the concentration of mature tRNA^{Asp} extrapolated to the y-intercept provides a good estimate of the burst amplitude (34 nM (85%)). The data at 20 nM RNase P RNA are fit to a burst mechanism (eq 3) with a single exponential, k_{burst} = 0.3 s^{-1} and amplitude = 16 nM (80%), followed by a linear phase, slope/[E] = 0.012 s^{-1}.

Scheme 1

$$E + \text{pre-tRNA} \underset{k_{-1}}{\overset{k_1}{\rightleftharpoons}} E\cdot\text{pre-tRNA} \xrightarrow{k_2} E\cdot 5'P\cdot\text{tRNA}$$

constant for the burst equal to 0.85 ± 0.1 mol of tRNA/mol of RNase P RNA and 0.3 ± 0.03 s^{-1}, respectively. The rate of the linear phase is consistent with the steady-state kinetic parameters measured under identical conditions (described later). These data demonstrate that the cleavage of pre-tRNA^{Asp} catalyzed by RNase P RNA is significantly faster than steady-state turnover and that ≥85% of the enzyme molecules are catalytically competent.

Pre-tRNA^{Asp} Association and Hydrolysis. The pre-tRNA binding and hydrolytic cleavage steps catalyzed by the RNA component of *B. subtilis* RNase P can be isolated by measuring a single turnover in the presence of excess enzyme ([E]/[S] ≥ 5). Under these conditions, product dissociation is not observable since E·tRNA and tRNA are indistinguishable on the denaturing polyacrylamide gels used for assaying cleavage. The reaction is initiated by mixing RNase P RNA and pre-tRNA^{Asp} in a quench-flow instrument and quenched by the addition of EDTA. A representative gel is shown in Figure 3. Identical results were obtained with a 5% trichloroacetic acid quench (data not shown). The time dependence of the appearance of tRNA^{Asp} at various concentrations of excess RNase P RNA is shown in Figure 4. At low concentrations of RNase P RNA (≤0.24 μM, Figure 4A), the appearance of tRNA^{Asp} is described by a single first-order exponential (eq 1) and the observed rate constant is linearly dependent on the concentration of RNase P RNA, with a slope of (3.3 ± 0.1) × 10^6 M^{-1} s^{-1}. However, at 1.4 μM RNase P RNA, there is a clear lag in product formation (Figure 4B). At high concentrations of RNase P RNA (*i.e.*, 19 μM, [E]/[S] ≥ 20), the lag almost disappears and the observed rate constant for product appearance is independent of the RNase P RNA concentration: k_{obs} = 5.3 ± 0.4 s^{-1} (fitting with a single exponential, eq 1) or 5.9 ± 0.3 s^{-1} (fitting with a double exponential, eq 2).

This is exactly the behavior expected for an irreversible pseudo-first-order reaction followed by an irreversible first-order reaction (Fierke & Hammes, 1994; Johnson, 1992) (Scheme 1, when $k_2 > k_{-1}$) in which the first step is the association of RNase P RNA and pre-tRNA^{Asp} to form a binary complex, k_1 = 3 × 10^6 M^{-1} s^{-1}, and the second step is the chemical cleavage step, k_2 = 5.9 s^{-1}. At low concentrations of RNase P RNA, the formation of E·pre-tRNA is slower than reaction of this intermediate (k_1[E] ≪ k_2), so that the formation of products essentially increases exponentially, with k_1[E] being the characteristic rate constant. At high concentrations of RNase P RNA (k_1[E] ≫ k_2), E·pre-tRNA rapidly accumulates, and the rate constant for formation of products essentially reflects the cleavage of bound substrate (k_2). At moderate concentrations of RNase P RNA (k_1[E] ≈ k_2), a "lag" in the formation of product is observed at short times, while the E·pre-tRNA intermediate is accumulating (k_1[E]) followed by an exponential decay of this intermediate (k_2). These data at intermediate concentrations of RNase P RNA are described by a double exponential (eq 2). The mechanism shown in Scheme 1 is sufficient to describe the appearance and disappearance of the lag. Furthermore, it is unlikely that the lag is due to alternative structures or multimers of RNase P RNA because it almost disappears at very high RNase P RNA concentrations.

To confirm the measurement of the association rate constant, the single-turnover experiments at low concentrations of RNase P RNA were repeated, except that the reaction was quenched by the addition of unlabeled tRNA prior to the addition of EDTA (Figure 5A). In the presence of high concentrations of tRNA, the noncovalent E·pre-tRNA complex can react to form products, although additional turnover is inhibited; therefore, the appearance of product reflects the rate of formation of E·pre-tRNA (Rose, 1980). This approach will be described in more detail in the following section. The data are described by a single first-order exponential (eq 1); the second-order rate constant for association, (6.3 ± 0.2) × 10^6 M^{-1} s^{-1}, is calculated from the slope of a plot of observed rate constant versus enzyme concentration (Figure 5B). The slight difference between this value of k_1 and the one obtained using a simple EDTA quench may be due to the formation of small amounts of E·pre-tRNA during the reaction. Finally, this association rate constant is consistent with the second-order rate constant measured from the pre-steady-state burst, (3.0 ± 0.5) × 10^6 M^{-1} s^{-1} (Figure 2), and is similar to that observed for the association of tRNA, (5.2 ± 0.8) × 10^6 M^{-1} s^{-1} (described later).

Dissociation of pre-tRNA^{Asp} from the E·S Complex. The kinetic mechanism in Scheme 1 predicts that a significant concentration of the E·pre-tRNA^{Asp} binary complex will build up at high concentrations of RNase P RNA (when k_1[E] > k_2). Furthermore, if $k_2 > k_{-1}$, then hydrolysis of the bound substrate to form tRNA^{Asp} and 5′P should be faster than dissociation of pre-tRNA^{Asp}. This can be tested by quenching the reaction with a high concentration of unlabeled tRNA ("tRNA trap") that will rapidly bind to any unbound RNase P RNA and inhibit further reaction with unbound labeled pre-tRNA^{Asp} (Rose, 1980). This method of quenching allows the intermediate enzyme complexes, such as E·pre-tRNA^{Asp}, to partition between dissociation (forming E + pre-tRNA^{Asp}) or cleavage (forming E + tRNA^{Asp} + 5′P) before the addition of EDTA. On the other hand, quenching with EDTA immediately chelates the magnesium ions required for cleavage, so that E·pre-tRNA^{Asp} is always observed as pre-tRNA^{Asp}. Therefore, if dissociation is slow relative to the cleavage step, E·pre-tRNA^{Asp} can be observed as product formed in the tRNA trap that is not observed in the EDTA quench, as shown in Figure 6.

At high concentrations of RNase P RNA, 90% of the pre-tRNA^{Asp} is cleaved after 25 ms in reactions stopped by the addition of excess unlabeled tRNA, followed by the addition

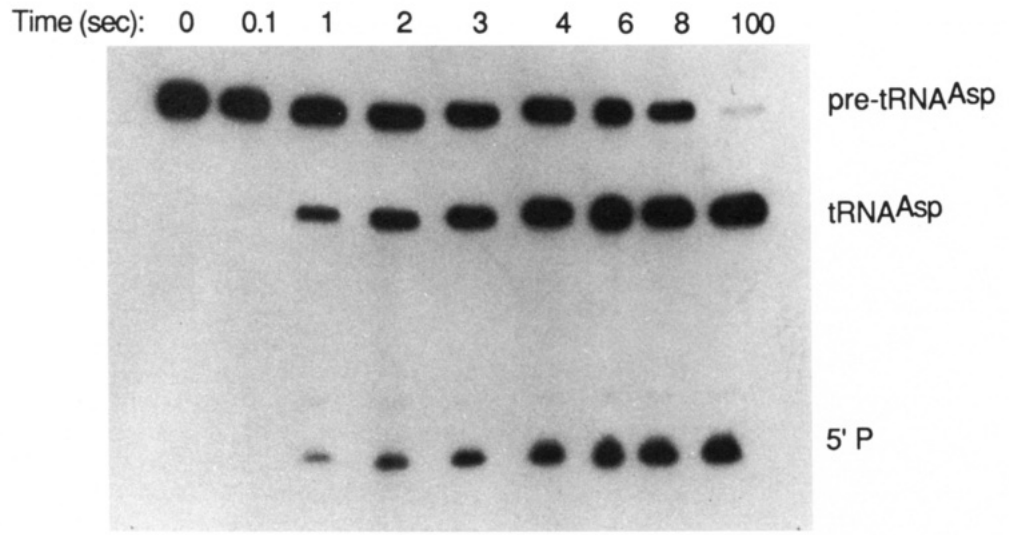

FIGURE 3: Gel (8% polyacrylamide/8 M urea) of the single-turnover reaction of 0.12 μM *B. subtilis* RNase P RNA with 0.026 μM pre-tRNA^{Asp}. The reaction was initiated by mixing the RNase P RNA component with pre-tRNA^{Asp} in a KinTek RQF3 quench-flow instrument and quenched at the indicated times by a 3-fold dilution into 90 mM EDTA followed by the addition of urea to 4 M. Reaction products were quantitated by scintillation counting of excised bands or by using a PhosphorImager from Molecular Dynamics.

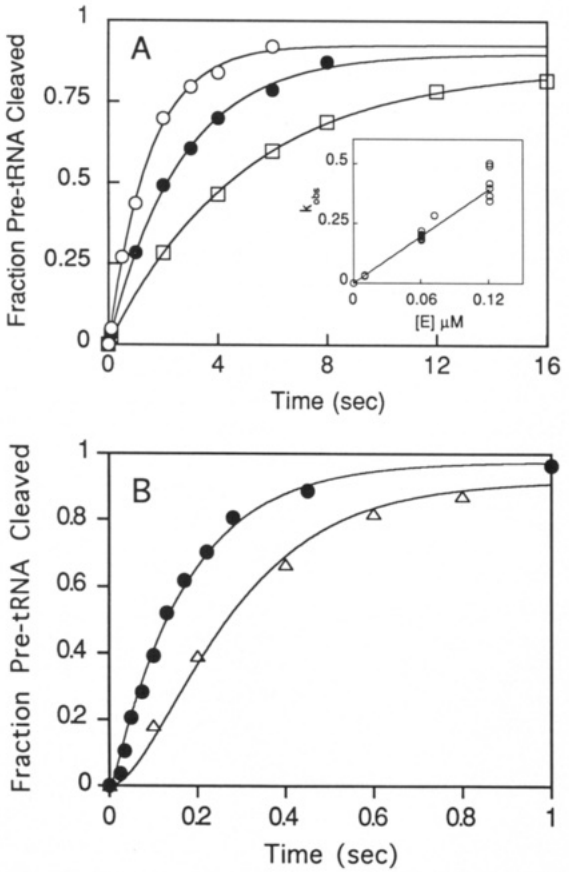

FIGURE 4: Single-turnover measurements of RNase P RNA-catalyzed hydrolysis of pre-tRNA^{Asp}. Pre-tRNA^{Asp} (0.024 μM) was mixed with varying concentrations of excess RNase P RNA in buffer 1 at 37 ° C and quenched with EDTA, and the reaction products were analyzed as described in the legend for Figure 3. (A) At low concentrations of RNase P RNA [0.06 (□), 0.12 (●), and 0.24 μM (○)], the data were fit by a single exponential. The inset shows the linear dependence of the observed first-order rate constant on the concentration of RNase P RNA with the slope = $(3.3 \pm 0.1) \times 10^6$ M^{-1} s^{-1}. (B) At higher concentrations of RNase P RNA [1.4 (△) and 19 μM (●)], the data were fit to a mechanism of two consecutive first- or psuedo-first-order reactions (eq 2) with $k_1 = 6 \times 10^6$ M^{-1} s^{-1} × [E] (see Figure 5) and $k_2 = 5.9 \pm 0.3$ s^{-1}.

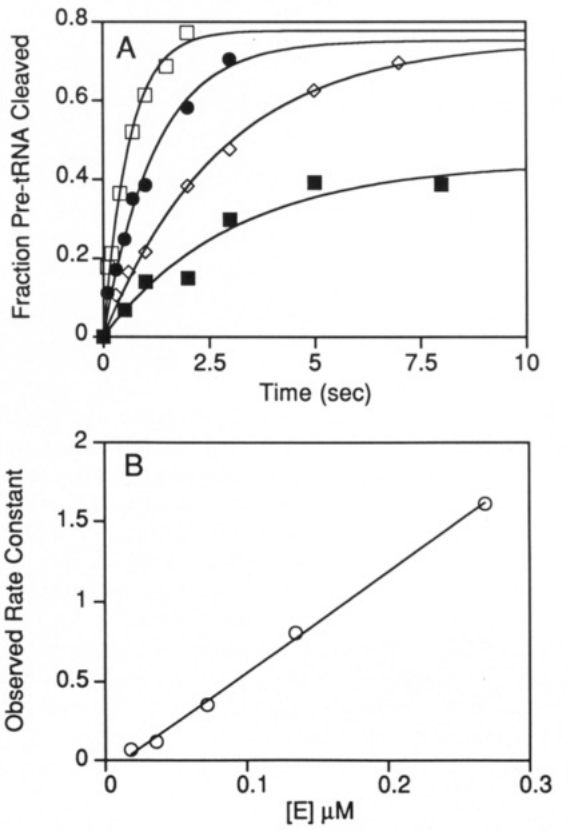

FIGURE 5: Single-turnover measurements of RNase P RNA-catalyzed hydrolysis of pre-tRNA^{Asp} quenched by the addition of unlabeled tRNA. (A) Pre-tRNA^{Asp} (0.012–0.024 μM) was mixed with varying concentrations of excess RNase P RNA [0.036 (■), 0.072 (◇), 0.13 (●), and 0.27 μM (□)] in a KinTek quench-flow apparatus in buffer 1 at 37 ° C and quenched by the addition of 2.1 vol of 58 μM unlabeled tRNA type XX. After incubation for 15–20 s, the reaction was stopped by the addition of EDTA and urea (final concentrations of 150 mM and 5 M, respectively). The reaction products were analyzed as described in the legend for Figure 3. Data were fit by a single first-order exponential. (B) The observed rate constants are linearly dependent on the enzyme concentration, with slope = $(6.3 \pm 0.2) \times 10^6$ M^{-1} s^{-1}.

of EDTA after 15 s; in contrast, <5% cleavage is observed in reactions quenched solely by EDTA. The tRNA trap data can be fit by a single exponential (eq 1) with the observed psuedo-first-order rate constant equal to $k_1[E] = 133 \pm 6$ s^{-1}, and the EDTA quench data can be described by this same step followed by an irreversible first-order rate constant of 5.9 s^{-1} (eq 2), as previously described (Figures 4B and 6). Taken together, these data clearly demonstrate that pre-tRNA^{Asp}

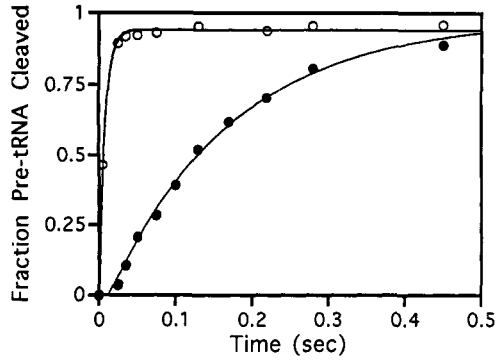

FIGURE 6: Formation of an E·pre-tRNA^{Asp} binary complex assayed by unlabeled tRNA trap. Pre-tRNA^{Asp} (0.024 μM) was mixed with excess RNase P RNA (19 μM) in a KinTek quench-flow instrument in buffer 1 at 37 °C. The reaction was quenched by 2.1 vol of either (●) 90 mM EDTA or (○) 58 μM unlabeled tRNA type XX, followed by the addition of an equal volume of 300 mM EDTA/10 M urea after 15–20 s. The reaction products were analyzed as described in the legend for Figure 3. The unlabeled tRNA trap data are fit by a single exponential, while the EDTA quench data are fit to a mechanism of two consecutive first-order (or pseudo-first-order) reactions (eq 2).

association (k_1) is fast with a rate constant $\approx 6 \times 10^6$ M^{-1} s^{-1}, and pre-tRNA^{Asp} dissociation from the E·S complex (k_{-1}) is significantly slower than the hydrolytic rate constant (k_2) of 6 s^{-1}. The rate constant for dissociation of pre-tRNA^{Asp} from the E·pre-tRNA^{Asp} binary complex (k_{-1}) was estimated at 0.5 ± 0.1 s^{-1} using the following equation (Rose, 1980):

$$[P]_{obs}/[P]_\infty = 0.926 = k_2/(k_2 + k_{-1}) \quad (8)$$

where $[P]_{obs}$ is the fraction of pre-tRNA cleaved at 25 ms (when [E·S] is maximal under these conditions) and $[P]_\infty$ is the end point of the reaction. Furthermore, simulation using the computer program HopKINSIM (Barshop et al., 1983; D. Wachsstock, personal communication) indicated that the cold trap data in Figure 6 were best described using $k_{-1} = 0.65 \pm 0.2$ s^{-1} with the kinetic scheme shown in Figure 1.

Equilibrium and Kinetic Constants for Product Binding. The previous experiments indicate that a step subsequent to pre-tRNA cleavage is the rate-limiting step for steady-state turnover catalyzed by RNase P RNA. To test whether this step is product dissociation, we measured or estimated the rate and equilibrium constants for the dissociation of both products, tRNA^{Asp} and 5′P. The E·tRNA^{Asp} complex was assayed from the decreased mobility of ^{32}P-labeled tRNA^{Asp} in a polyacrylamide gel upon complexation with the RNA component of RNase P, as shown in Figure 7A (Hardt et al., 1993; Pyle et al., 1990). This method is applicable even at the very high concentrations of salt used in this experiment, although it is essential that the ionic strength and magnesium concentration of the running and gel buffers are identical to those of the equilibration buffer. The dissociation constant for this binary complex, $K_D = 2.5 \pm 0.5$ nM (Figure 7B), was determined from the concentration dependence of this mobility shift in buffer 1 at 37 °C. These data do not demonstrate any cooperativity in binding tRNA^{Asp} to *B. subtilis* RNase P RNA, as has been proposed for binding tRNA^{Gly} to *E. coli* RNase P RNA (Hardt et al., 1993).

Additionally, the E·tRNA^{Asp} complex was separated from unbound tRNA^{Asp} on a Sephadex G-75 centrifuge column (Penefsky, 1979; Sambrook et al., 1989); quantitation of the bound complex as a function of the RNase P RNA concentration confirmed that the $K_D = 3.2 \pm 0.4$ nM (Figure 7B). This is the first application of this method for quantifying RNA–RNA association energies. The short time required for separation of the complex from the unbound RNA and the ease of performing experiments at many different conditions simultaneously may provide significant advantages over gel shift and gel filtration assays (Hardt et al., 1993; Pyle et al., 1990; Pyle & Green, 1994). This technique is also useful for measuring dissociation and association rate constants, as will be described later.

Scheme 2

$$E{\cdot}5'P + tRNA \overset{K_D^{5'P}}{\rightleftharpoons} 5'P + E + tRNA \overset{K_D^{tRNA}}{\rightleftharpoons} E{\cdot}tRNA + 5'P$$

The K_D for the 5′ product was estimated as 0.43 ± 0.09 μM from the decrease in k_{obs} for RNase P RNA-catalyzed cleavage of pre-tRNA^{Asp} under single-turnover conditions (see Figure 4A) as a function of the concentration of 5′P (data not shown). The gel shift assay was used to estimate the dissociation constants of 5′P and tRNA from the ternary product complex, E·5′P·tRNA. In this experiment, the observed dissociation constant for tRNA increases linearly with increasing concentration of 5′P (Figure 7C). One possible explanation for these data is that the binding of 5′P and tRNA in the binary complexes is competitive (Scheme 2); in other words, they both bind to the same or overlapping binding sites. This suggests that the binding of 5′P in the binary complex is nonproductive and should act to inhibit turnover. However, 5′P may also bind to form *productive* binary (E·5′P) and ternary (E·tRNA·5′P) complexes without affecting the dissociation constant of tRNA, and therefore, we would not observe the formation of these complexes using this technique. A second explanation for the increase in K_D^{tRNA} in the presence of 5′P is that tRNA and 5′P display significant negative cooperativity in binding at the correct sites. In this case, since the plot of the observed K_D for tRNA versus [5′P] shows no curvature at high concentration, indicative of the formation of a ternary complex, the dissociation constant for the binding of tRNA to E·5′P is $\gg 1.5$ μM.

The rate constant for dissociation of a ligand from a binary complex with RNase P RNA can be measured by a competition experiment. In this technique, the enzyme–^{32}P-labeled tRNA (E·tRNA*) complex is mixed with a large excess of unlabeled tRNA^{Asp}, which competes for the binding site. The concentration of E·tRNA* versus time is monitored by radioactivity in the eluate of a Sephadex G-75 centrifuge column, which separates the bound and free tRNA* faster than tRNA* dissociates from the complex. When the binding of tRNA to RNase P RNA is much faster than the dissociation of tRNA* (k_1[tRNA] $\gg$ k_{-1}), the observed rate constant for the disappearance of E·tRNA* is equal to the dissociation rate constant for tRNA. This condition is met when the concentration of unlabeled tRNA^{Asp} is $\geq$30 nM, given the previously measured dissociation constant of 3 nM and the association and dissociation rate constants described here. The time-dependent disappearance of E·tRNA^{Asp}* (Figure 8A) yields a dissociation rate constant for tRNA^{Asp}, $k_{off} = 0.013 \pm 0.002$ s^{-1} (eq 4), that is similar to the steady-state turnover at high pre-tRNA^{Asp} ($k_{cat} = 0.019 \pm 0.001$ s^{-1}), demonstrating that dissociation of tRNA from E·tRNA is the rate-limiting step for turnover. On the other hand, dissociation of 5′P from the E·5′P binary complex occurs during the transit time of the column ($\leq$10 s), demonstrating that $k_{off} \geq 0.2$ s^{-1}. These rate constants suggest a kinetically preferred pathway of product dissociation: 5′P dissociates from the E·tRNA·5′P ternary complex first followed by dissociation of tRNA.

The rate of formation of the E·tRNA complex was monitored as the appearance of radioactivity in the eluate of a Sephadex G-75 centrifuge column after mixing ^{32}P-labeled tRNA^{Asp} with RNase P RNA. Under pseudo-first-order

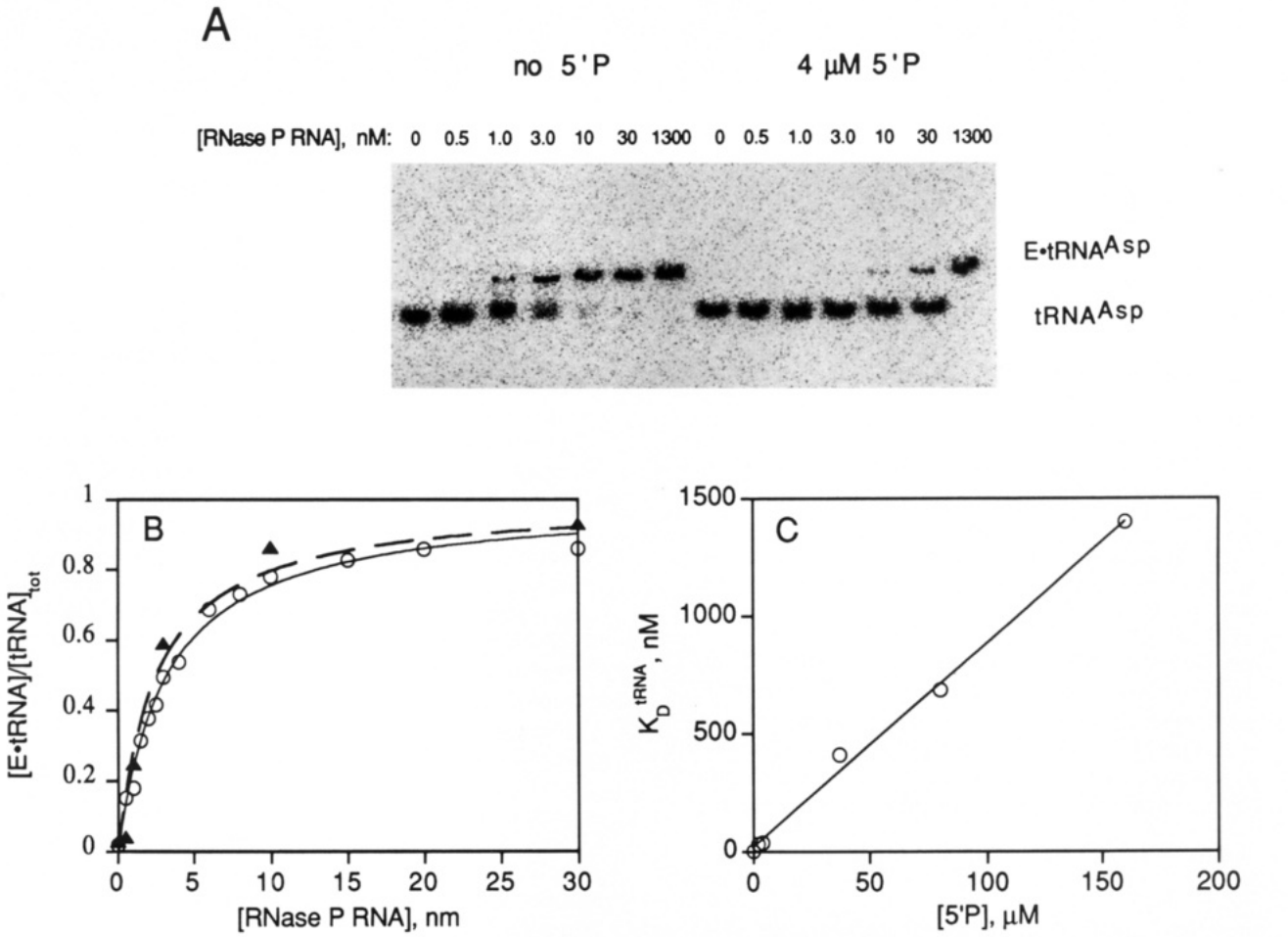

FIGURE 7: Measurement of the dissociation constant for $tRNA^{Asp}$. (A) Representative 10% polyacrylamide gel from a gel shift experiment. ^{32}P-labeled $tRNA^{Asp}$ (0.1 nM) was incubated with RNase P RNA (1–1300 nM) under standard conditions for 1 h. Some of the reaction mixtures also contained 4 μM 5′P (lanes 8–14). These samples were then loaded onto a 10% polyacrylamide gel, where the gel and running buffer contained 50 mM Tris–acetate (pH 8.0), 100 mM magnesium acetate, 800 mM NH_4Cl, and 0.1 mM EDTA, and the temperature was maintained at 37 °C. The mobility of ^{32}P-labeled $tRNA^{Asp}$ decreased with increasing concentrations of RNase P RNA in the reaction mixture, reflecting the formation of an E·tRNA complex. The bound and free $tRNA^{Asp}$ were quantitated using a PhosphorImager from Molecular Dynamics. (B) RNase P RNA (0–1.3 μM) was incubated with ^{32}P-labeled $tRNA^{Asp}$ (0.1 nM) in buffer 1 at 37 °C. The fraction of $tRNA^{Asp}$ bound to RNase P RNA was assayed either by decreased mobility in a 10% polyacrylamide gel (▲, dashed line) or by radioactivity in the eluate of a Sephadex G-75 centrifuge column (○, solid line) (carried out as described in the Materials and Methods section) as a function of the concentration of the RNA component of RNase P. Using eq 5, the data were fit with a K_D of 2.5 ± 0.5 or 3.2 ± 0.4 nM from the gel shift and centrifuge column experiments, respectively. (C) The K_D^{tRNA} was measured at several concentrations of 5′P (0–160 μM) using the gel shift technique. The linear increase in K_D^{tRNA} as a function of added 5′P indicates that these two products compete for the same binding site or display negative cooperativity, showing no evidence of formation of a stable E·5′P·$tRNA^{Asp}$ ternary complex.

conditions ($[E]/[tRNA^{Asp}] \geq 5$), the appearance of the binary complex is described by a single first-order exponential (eq 1), which is dependent on the concentration of RNase P RNA (Figure 8B). For a simple association reaction, the observed rate constant under pseudo-first-order conditions may be approximated by $k_{obs} = k_{on}[E] + k_{off}$, where k_{on} and k_{off} are the association and dissociation rate constants, respectively. In a linear plot of k_{obs} versus [E] (Figure 8B, inset), the slope is $k_{on} = (5.2 \pm 0.9) \times 10^6$ M^{-1} s^{-1} and the intercept is $k_{off} = 0.013 \pm 0.002$ s^{-1}. These data are consistent with a simple association step for tRNA. The k_{off} is identical to the dissociation rate constant measured from the competition experiment, and the ratio of the rate constants ($k_{off}/k_{on} = 2.5$ nM) is consistent with the K_D measured for the formation of E·$tRNA^{Asp}$.

Comparison of Pre-Steady-State and Steady-State Data. These experiments define a scheme that describes the kinetic behavior of a single turnover catalyzed by the RNA component of RNase P (steps shown in heavy arrows in the kinetic scheme in Figure 1). An essential test of this kinetic scheme is whether it describes the observed steady-state kinetic parameters. The maximal rate constant for cleavage of pre-$tRNA^{Asp}$ by the RNA component of RNase P, $k_{cat} = 0.019$ s^{-1}, is identical, within experimental error, to the observed dissociation rate constant for $tRNA^{Asp}$, as predicted by the scheme in Figure 1. However, the steady-state parameter measuring the second-order reaction of the RNA component of RNase P with pre-$tRNA^{Asp}$, $k_{cat}/K_M = 1.6 \times 10^5$ M^{-1} s^{-1} (eq 6), is about 40-fold slower than the rate constant predicted by this kinetic scheme, $k_{cat}/K_M = k_{on}^{pre\text{-}tRNA} = 6.3 \times 10^6$ M^{-1} s^{-1}. This difference does not simply reflect differences in experimental conditions; we have measured both the pre-steady-state binding step and the steady-state k_{cat}/K_M in a single-burst experiment (see Figure 2). Since single-turnover experiments measure the formation of E·P (E + S → E·P) but not the turnover of RNase P RNA (E·P → E), the simplest model consistent with these data is that a novel enzyme species (E′) is produced during the first turnover that binds substrate significantly more slowly and does not equilibrate rapidly with the original conformer (E). This additional step has been incorporated into our minimal kinetic scheme shown in Figure 1.

Further Evidence for the Novel Enzyme Species. This model predicts that at very low substrate concentrations the observed rate constant for binding pre-tRNA to E′ should become slower than the rate constant for conversion from E′ to E. At these substrate concentrations, the initial velocity

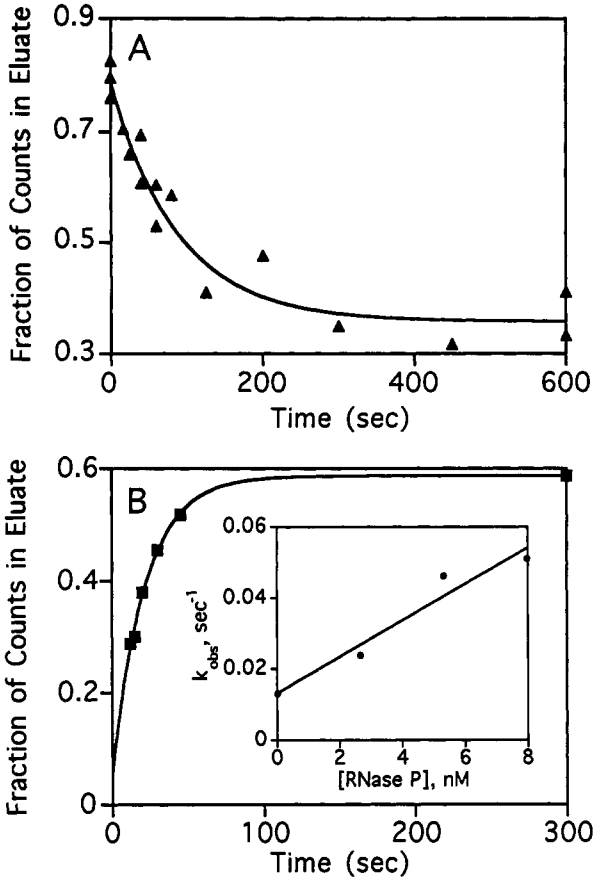

FIGURE 8: Binding kinetics for the formation of a binary complex between tRNA^{Asp} and the RNA component of RNase P. (A) Rate constant for the dissociation of tRNA^{Asp} from the E·tRNA complex. ^{32}P-labeled tRNA^{Asp} (0.1 nM) was incubated with RNase P RNA (30 nM) under standard conditions for 1 h to form the binary complex. Dissociation of labeled tRNA^{Asp} was observed by the addition of unlabeled gel-purified tRNA^{Asp} (100 nM). The E·[^{32}P]tRNA^{Asp} binary complex was monitored by the radioactivity in the eluate of a Sephadex G-75 centrifuge column run as described in the Materials and Methods section. The data are fit by a single exponential decay (eq 4). (B) Association rate constant for the formation of E·tRNA^{Asp}. ^{32}P-labeled tRNA^{Asp} (0.5 nM) was mixed with excess RNase P RNA (5.4 nM), and the formation of the binary complex was monitored by the radioactivity in the eluate of a Sephadex G-75 centrifuge column. The data are fit by a single first-order exponential. The inset shows a plot of k_{obs} for formation of the binary complex as a function of [E]. The slope of this plot is $k_{on} = (5.2 \pm 0.8) \times 10^6$ M^{-1} s^{-1} and the intercept is $k_{off} = 0.013 \pm 0.002$ s^{-1}.

for the reaction should reflect binding of pre-tRNA to E, such that $k_{cat}/K_M = 6.3 \times 10^6$ M^{-1} s^{-1}. Indeed, curvature is observed in a plot of the initial rate for pre-tRNA cleavage versus the concentration of pre-tRNA^{Asp} at concentrations significantly below the K_M (≤0.03 μM) (Figure 9, inset). This downward curvature at higher substrate concentrations is not due to substrate inhibition since the reaction velocity is constant at much higher concentrations of pre-tRNA^{Asp} (1–20 μM), nor is the curvature caused by aggregation of RNase P RNA or an inhibitor in the enzyme preparation since the enzyme concentration is constant for most of the steady-state reactions.

The concentration dependence of steady-state turnover (Figure 9) can not be described by the Michaelis–Menten equation because there are two concentration-dependent phases. When these data are fit to the Michaelis–Menten equation (eq 6), at low [pre-tRNA^{Asp}] the fitted line is linearly dependent on substrate concentration and significantly underestimates the observed rate. However, the observed steady-state data can be fit by eq 9, which was derived from the scheme shown in Figure 1 (Segel, 1975). This kinetic mechanism includes slow equilibration between two enzyme

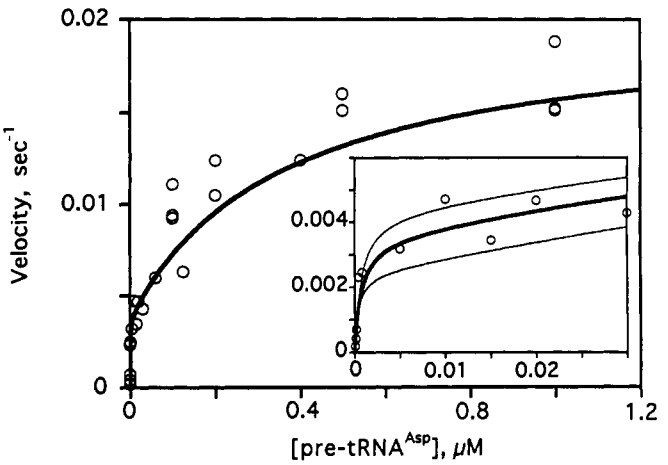

FIGURE 9: Reaction velocity versus pre-tRNA^{Asp} concentration under steady-state conditions. RNase P RNA (2 nM or [S]/[E] ≥ 5 when the substrate concentration was ≤10 nM) was mixed with excess pre-tRNA^{Asp} (0.03–1000 nM) in buffer 1 at 37 °C. At various times the reaction was quenched by the addition of an equal volume of 200 mM EDTA (pH 8.0)/10 M urea. The initial velocity (<10% hydrolysis) was calculated from the slope of a plot of [tRNA] versus time. The inset shows data at substrate concentrations of ≤0.03 μM. The data are fit using eq 9. Data are weighted assuming 20% error, as determined from the average standard deviation of multiple (≥3) data points. The rate constants for interconversion between E and E′ were estimated by fitting the data after the insertion of all of the other rate constants shown in Figure 1. The thin lines represent simulations of the data where k_5 is set at 0.0054 (upper line) and 0.0034 s^{-1} (lower line) with all of the other rate constants held constant.

conformers with a decreased association rate constant for pre-tRNA^{Asp} binding to one of the conformers, leading to the higher order dependence on substrate concentration. When steady-state data at various concentrations of pre-tRNA^{Asp} (0.03–1000 nM) are fit to this equation (eq 9, Figure 9), the rate of the reaction is defined by $(k_{cat}/K_M)_1 = A/C = (4.8 \pm 0.8) \times 10^6$ M^{-1} s^{-1}, measuring the association of E and S (for [S] ≤ 0.8 nM), $(k_{cat}/K_M)_2 = B/D = (6.9 \pm 2.2) \times 10^4$ M^{-1} s^{-1}, representing the binding of E′ and S (for 5.0 nM ≤ [S] ≤ 30 nM), and $k_{cat} = B/E = 0.021 \pm 0.003$ s^{-1}, reflecting the rate constant for tRNA dissociation ([S] > 1 μM). $(k_{cat}/K_M)_2$ is smaller than the $k_{cat}/K_M = (1.6 \pm 0.03) \times 10^5$ M^{-1} s^{-1} determined previously from fitting steady-state data to eq 6, because this equation forces the line through the origin. However, k_{cat} is unaffected.

$$\text{rate} = (A[S] + B[S]^2)/(C + D[S] + E[S]^2) \qquad (9)$$

where

$$A = k_2k_3k_4(k_1k_5 + k_{-5}k_6)$$

$$B = k_1k_2k_3k_4k_6$$

$$C = k_2k_3k_4(k_5 + k_{-5})$$

$$D = k_4[k_3(k_1k_5 + k_1k_2 + k_{-5}k_6 + k_{-1}k_6) + k_1k_2k_5 + k_2k_{-5}k_6] + k_2k_3(k_1k_5 + k_{-5}k_6)$$

$$E = k_1k_6(k_2k_4 + k_2k_3 + k_3k_4)$$

The rate and equilibrium constants for conversion between E and E′ were also estimated from fitting the data in Figure 9 to eq 9, with all of the other rate constants defined as shown in Figure 1. The conversion of E′ to E is slow, $k_5 = 0.0044 \pm 0.001$ s^{-1}, and the equilibrium formation of E′ is unfavorable, $k_{-5}/k_5 = 0.3 \pm 0.1$. Simulation of the data using eq 9 with the rate constants in Figure 1 and varying k_5 from 0.0034 to

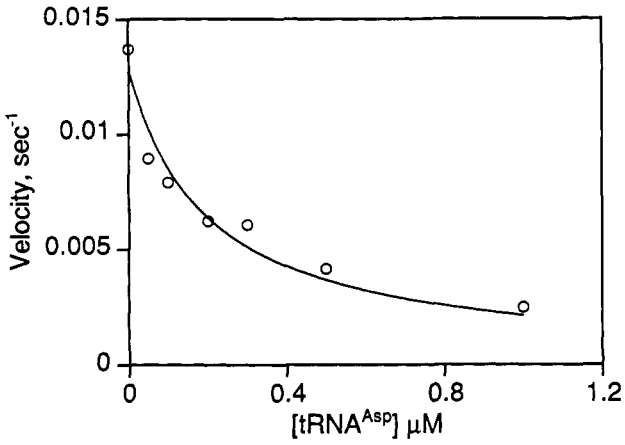

FIGURE 10: Inhibition of steady-state turnover as a function of the concentration of tRNA^{Asp}. RNase P RNA (2 nM) was incubated for 1 h with various concentrations of tRNA^{Asp} (0–1 μM) in buffer 1 at 37 °C. Turnover was initiated by the addition of pre-tRNA^{Asp} (100 nM), and the reaction was quenched at various times by the addition of an equal volume of 200 mM EDTA and 10 M urea. The initial velocity was calculated from the slope of a plot of [tRNA] versus time. The data are fit assuming competitive inhibition (eq 7) with K_I = 0.11 ± 0.02 μM and $K_M = 1.1 \times 10^{-7}$ M.

0.0054 s^{-1} (see Figure 9, inset) demonstrates that the maximum rate constant of the first substrate-dependent phase is sensitive to the value of k_5. However, the overall fit is not very sensitive to the value of the equilibrium constant (k_{-5}/k_5) as long as it is ≤0.3. Additionally, simulation of the burst data (Figure 2) using HopKINSIM and the kinetic scheme in Figure 1 indicates that k_{-5}/k_5 must be ≤0.1 to obtain the observed burst amplitude of >80%. Therefore, the actual rate constant for conversion of E to E′ is likely $k_{-5} \leq 0.0004$ s^{-1}.

Finally, to test whether the E′ conformer of RNase P RNA also binds mature tRNA^{Asp} less tightly, we measured the inhibition constant, K_I, for tRNA^{Asp} for steady-state turnover at 0.1 μM pre-tRNA^{Asp}. At this substrate concentration, E′ accumulates and binds substrate faster than interconversion to the E conformer (Figure 1). The initial velocity for hydrolysis of pre-tRNA^{Asp} (0.1 μM) catalyzed by the RNA component of RNase P (2.0 nM) in buffer 1 at 37 °C decreased hyperbolically with increased tRNA^{Asp} concentration. Fitting this data with eq 7 and assuming that tRNA^{Asp} acts as a competitive inhibitor (Smith et al., 1992) indicates that K_I is 0.11 ± 0.02 μM (Figure 10). This inhibition constant is significantly larger than the measured K_D of about 3 nM (Figure 7B), indicating that E′ also binds tRNA less tightly.

Overall Equilibrium Constant. To determine a lower limit for the equilibrium constant for pre-tRNA^{Asp} hydrolysis, we incubated 0.09 μM tRNA^{Asp} with 9 nM RNase P RNA and either 1.02 mM 5′P or 17 mM ATP. In both cases, ≤0.36 nM substrate was formed, indicating that the equilibrium constant was ≥0.26 M or 10 M, respectively. ATP was added in an attempt to observe religation because RNase P RNA is capable of cleaving a pre-tRNA molecule with a single nucleotide replacing the 5′ fragment (Smith & Pace, 1993). To demonstrate that these reactions reached equilibrium, a small amount of labeled pre-tRNA was added that was completely cleaved within 2 h. This estimated equilibrium constant is consistent with values measured for the hydrolysis of simple phosphate esters, which range from approximately 30 M for adenosine monophosphate to 5000 M for glucose 1-phosphate (Williams & Lansford, 1967). Furthermore, the kinetic mechanism shown in Figure 1 is consistent with these values for the overall equilibrium constant.

DISCUSSION

Summary of the Kinetic Mechanism. Investigation of the catalytic mechanism of RNase P RNA has been limited by the inability to assign changes in the observed rate to individual reaction steps. Therefore, we have measured various association and dissociation rate constants and the rate constant for the cleavage step catalyzed by the RNA component of *Bacillus subtilis* RNase P. These experiments have led to the formulation of a minimal kinetic mechanism for RNase P RNA (Figure 1) that describes the kinetic behavior of this enzyme under both steady-state and pre-steady-state conditions. In this mechanism, the association and dissociation rate constants for pre-tRNA^{Asp} binding to the E conformer (k_1 and k_{-1}) have been measured directly from single-turnover, tRNA trapping, and pre-steady-state experiments. Furthermore, the rate constant for cleavage of pre-tRNA^{Asp} (k_2) was determined from single-turnover experiments at high RNase P RNA concentrations. The simplest mechanism is that this rate constant measures phosphodiester bond hydrolysis since there is no evidence for an additional step, such as a conformational change. Moreover, this cleavage rate constant is likely pH dependent since the hydrolysis of pre-tRNA^{Asp} under single-turnover conditions is 160-fold slower at pH 6 (Smith & Pace, 1993). Additional evidence for a rate-limiting chemical step could be obtained by measuring the rate constant for hydrolysis of pre-tRNA containing a phosphorothioate at the cleavage site (Herschlag et al., 1991; Herschlag & Khosla, 1994). In the reverse direction, we did not observe the formation of pre-tRNA^{Asp} due to religation. However, cleavage of pre-tRNA^{Asp} is nearly complete (>95%) in single-turnover reactions, indicating that the rate constant for religation (k_{-2}) must be slower than the rate constant for dissociation of 5′P from the ternary product complex ($k_3 \geq 0.2$ s^{-1}). A kinetic mechanism including pre-tRNA association, hydrolysis, and dissociation of 5′P is sufficient to describe all of the single-turnover kinetic data.

The additional steps shown in Figure 1 are required to describe the steady-state kinetic behavior of RNase P RNA. For steady-state turnover under k_{cat} conditions, the kinetic mechanism is as follows: (1) substrate binds to the E′ conformer; (2) pre-tRNA^{Asp} is hydrolyzed at a specific position to form mature tRNA^{Asp} and the 5′P fragment; and (3) product dissociation occurs in a kinetically ordered pathway with dissociation of 5′P followed by dissociation of tRNA, leaving RNase P RNA in the E′ conformer. Comparison of the rate constant for tRNA dissociation to k_{cat} indicates that the rate-limiting step for steady-state turnover is the dissociation of tRNA (k_4) with all of the other rate constants at least 2-fold larger. Furthermore, the formation of a second, slowly exchanging enzyme conformer (E′) during turnover is required to explain the observed k_{cat}/K_M that is slower than the association rate constant for pre-tRNA^{Asp} and the higher order dependence of steady-state turnover on substrate concentration. At very low pre-tRNA concentrations, k_{cat}/K_M reflects binding of S to the E conformer with the observed association rate constant of 6×10^6 M^{-1} s^{-1}. The rate and equilibrium constants for exchange between the two enzyme conformers (k_5 and k_{-5}) were estimated from fitting the steady-state turnover rate as a function of pre-tRNA^{Asp} concentration (Figure 9).

In Figure 1, we present a minimal scheme necessary to explain our current data; therefore, we do not include any binary or ternary complexes with the novel E′ conformer. However, it is likely that binding of pre-tRNA^{Asp} and/or tRNA to E′ occurs in a two-step process (shown in Scheme 3), including an encounter complex followed by a conformational

Scheme 3

$$E' + S \underset{k_{-i}}{\overset{k_i}{\rightleftharpoons}} E'\cdot S \underset{k_{-ii}}{\overset{k_{ii}}{\rightleftharpoons}} E\cdot S$$

change. In this case, the decreased association rate constant observed for pre-tRNA^{Asp} binding to the E′ conformer reflects both binding to E′ and a conformational change [$k_6 = k_i k_{ii}/(k_{-i} + k_{ii})$, assuming that $k_{-ii} < k_2$]. This is also implied for tRNA and 5′P binding to E′ by the decrease in K_I compared to K_D (Figure 10 and unpublished data). Similarly, k_{-6} includes the rate constants for both dissociation of pre-tRNA^{Asp} and a conformational change; however, the value for k_{-6} is not constrained by our data as long as it is less than k_2. The kinetic mechanism shown in Figure 1 is sufficient to explain all of the steady-state and transient kinetic data, providing an excellent starting point for further mechanistic studies of RNase P.

Hydrolytic Step. Although the minimal kinetic scheme described in Figure 1 is the first complete kinetic mechanism determined for RNase P RNA, previous experiments have isolated some individual rate constants. Single-turnover experiments have been used to estimate a hydrolytic rate constant of 0.14 s^{-1} for cleavage of the pre-tRNA^{Tyr}su3 catalyzed by the RNA component of RNase P from *E. coli* (Tallsjö & Kirsebom, 1993). This rate constant is 43-fold lower than the one presented here under almost identical buffer conditions, $k_2 = 6$ s^{-1}, and reflects the decreased efficiency of either or both the pre-tRNA^{Tyr}su3 substrate and the *E. coli* RNase P RNA. However, our cleavage rate constant is similar to the value of 3 s^{-1} (pH 8) for hydrolysis of pre-tRNA^{Asp} catalyzed by the RNA component of *E. coli* RNase P estimated by extrapolation from the single-turnover rate constant at pH 6 (Smith & Pace, 1993). In these previous studies, the single-turnover data were analyzed assuming rapid equilibrium formation of the E·pre-tRNA noncovalent complex ($k_{-1} > k_2$) which, at least under our conditions, is not a valid assumption (see Figures 4B and 6) and underestimates the rate constant for cleavage (k_2).

This kinetic mechanism provides information that may be utilized to compare the catalytic rates of RNase P to those of other enzymes. The turnover rate of RNase P is slow compared to those of many enzymes, including triosephosphate isomerase (Albery & Knowles, 1976), carbonic anhydrase (Silverman & Lindskog, 1988), and dihydrofolate reductase (Fierke et al., 1987a), that operate at high catalytic efficiency as a consequence of evolution. This suggests that RNase P has been optimized for cleavage site selectivity and heterogeneous substrate recognition, not for rapid catalysis. This is similar to the result obtained for DNA polymerases, which are optimized for their fidelity of replication, not their catalytic efficiency (Fierke et al., 1987b). The hydrolytic rate constant is very similar to that measured for the *Tetrahymena thermophila* ribozyme using the 3′-OH of a bound guanosine as a nucleophile (6 s^{-1} for RNase P RNA and *T. thermophila* ribozyme) (Herschlag & Cech, 1990). The RNA component of RNase P catalyzes hydrolysis significantly faster than other ribozymes; estimations of the hydrolytic rate constants are 0.01 s^{-1} for the *Tetrahymena thermophila* ribozyme (Herschlag & Cech, 1990) and ≈0.001 s^{-1} for a group II intron ribozyme (Pyle & Green, 1994). This is reasonable since RNase P RNA is the only ribozyme of this group that has been optimized by evolution to catalyze hydrolytic reactions.

Association and Dissociation Rate Constants. Previous estimates of the rate constant for association of pre-tRNA^{Asp} and RNase P RNA derived from steady-state kinetic parameters (Smith & Pace, 1993) are an order of magnitude slower than our measurements using transient kinetics and are consistent with binding to the E′ conformer rather than the E conformer. Association rate constants for binding substrates and products to the E conformer are faster, approximately 5×10^6 M^{-1} s^{-1}. Although slower than the estimated diffusion limit of 10^8 M^{-1} s^{-1}, these rate constants are comparable to those of most protein enzymes (Hammes, 1982; Fersht, 1985) and slightly faster than those measured for the *Tetrahymena thermophila* ribozyme ($k_{on} \approx 1 \times 10^6$ M^{-1} s^{-1}) and hammerhead ribozymes ($(0.15–1.4) \times 10^6$ M^{-1} s^{-1}). The association steps in these ribozymes have been interpreted as dominated by helix formation and tertiary interactions (Herschlag & Cech, 1990; Herschlag, 1992; Fedor & Uhlenbeck, 1992). In fact, measurement of substrate binding to the *Tetrahymena thermophila* ribozyme is indicative of two kinetic phases (Young et al., 1991; Herschlag, 1992; Bevilaqua et al., 1992). These data are consistent with two-step binding in which base pairing forms in a bimolecular step ($k_{on} = 4 \times 10^6$ M^{-1} s^{-1}) followed by the formation of tertiary contacts. A variety of data, including the variability in pre-tRNA sequence, suggest that the RNA·RNA interaction in the RNase P·pre-tRNA binary complex does not involve base pairing. It is more likely that the overall structure of pre-tRNA is the main information used by RNase P in selecting its substrates, as indicated by the positions of chemically modified residues in tRNA that inhibit activity (Thurlow et al., 1991), the requirement for the amino acid acceptor stem and the T stem and loop in model substrates to observe catalytic activity (McClain et al., 1987), and a positive correlation between mutations that disrupt the secondary structure of tRNA and those that prevent pre-tRNA processing (Pace & Smith, 1990).

The rate-limiting step for multiple turnovers catalyzed by the RNase P RNA component is product dissociation ($k_{cat} = 0.02$ s^{-1}). This has previously been observed for many protein enzymes (Fersht, 1985) and also for the *T. thermophila* ($k_{cat} = 0.002$ s^{-1}) and long hammerhead ribozymes (≈0.001 s^{-1}) (Herschlag & Cech, 1990; Fedor & Uhlenbeck, 1992), although the cleavage step appears to be rate limiting for multiple turnovers for a group II intron ribozyme (Pyle & Green, 1994). When product release is rate-limiting, the kinetic parameters for steady-state turnover provide little information about either the catalytic mechanism or substrate binding (since K_M *does not* equal K_D). Furthermore, variations in either the solution conditions or the structure of the enzyme or substrate can cause changes in the steady-state rate-limiting step, as observed in RNase P RNA and dihydrofolate reductase (Smith et al., 1992; Mayer et al., 1986), making detailed mechanistic studies using steady-state kinetics even more difficult. Therefore, measuring the rate constants for individual steps is an essential tool for delineating the catalytic mechanism of this enzyme.

Conformational Change. Our data indicate that a second conformer of RNase P RNA, E′, forms during the first turnover. This conformer is less stable than the conformer obtained by preincubation at 37 °C ($[E']/[E] \leq 0.1$), and conversion to E is slow ($k_{obs} = 0.004$ s^{-1}). Our data suggest that a main kinetic difference between these two conformers is a decreased association rate constant for binding substrates, and likely for products as well. Product dissociation appears to be unaffected since the observed rate constant does not depend on whether E·tRNA is formed by the addition of tRNA^{Asp} or pre-tRNA^{Asp}. Finally, if interconversion between the two conformers occurs in the binary complexes, E·S ↔ E′·S, it must be significantly faster than k_4 (0.02 s^{-1}) or k_{cat} would be slower than product dissociation. The E′ conformer

could vary in RNA conformation, bound metals, or bound products. However, the fact that k_{cat}/K_M is independent of the ratio of enzyme to substrate makes this latter explanation unlikely. Lags in steady-state turnover in the absence of preincubation steps (Altman & Guerrier-Takada, 1986) and the observation of multiple tRNA binding constants (Hardt et al., 1993) have been interpreted as indicating conformational mobility in RNase P RNA. However, there may be multiple conformers of RNase P RNA, and there is currently no evidence indicating that the E′ conformer is present in the absence of preincubation. Since RNase P holoenzyme has a k_{cat}/K_M for steady-state turnover similar to the rate constant for binding pre-tRNA^{Asp} to the E conformer, ($\approx 4 \times 10^6$ M^{-1} s^{-1}; Reich et al., 1988), we speculate that an important role for the protein component is either to inhibit formation of the E′ conformer during turnover or to catalyze equilibration between the two conformers. It is possible that the high salt necessary to observe multiple turnovers also affects the E′/E equilibrium. We are currently testing these models as well as attempting to isolate and biochemically characterize RNase P RNA in the E′ conformer.

Conformational changes have also been observed in binding oligomers to the *T. thermophila* ribozyme (Bevilacqua, 1992; Herschlag, 1992), with a second, distinct conformational change observed subsequent to (or associated with) binding the guanosine cofactor (Herschlag & Khosla, 1994). These data suggest that conformational changes are fundamental steps on the catalytic pathway of many ribozymes. Further investigation of the conformational change in RNase P RNA will provide information about the structure and dynamics of catalytic RNAs and the role of conformational changes in catalysis.

Future Studies. This study defines a minimal kinetic scheme for the hydrolysis of pre-tRNA^{Asp} catalyzed by the RNA component of *B. subtilis* RNase P under high salt conditions. This scheme allows us to measure association, dissociation, hydrolytic, and conformational steps directly and will allow us to pinpoint the role of metals, pH, and the protein component in each step of the reaction. This is not currently possible using steady-state kinetic techniques since pre-tRNA association and tRNA dissociation are the rate-limiting steps in k_{cat}/K_M and k_{cat}, respectively. Furthermore, it is a necessary background for interpreting the effect of primary sequence changes in both the substrate and enzyme on catalytic activity. This is essential for identifying the active site of RNase P and for comprehending the rules governing molecular recognition in this enzyme. These additional studies should lead to a greater understanding of the chemistry and mechanisms of rate acceleration utilized by ribozymes.

ACKNOWLEDGMENT

We thank Dr. Daniel Herschlag, Dr. Michael Been, Dr. Norman Pace, and each of their respective laboratories for providing helpful advice. We also thank the laboratory of Dr. Norman Pace for providing useful plasmids.

REFERENCES

Abelson, J. (1979) *Annu. Rev. Biochem. 48*, 1035.
Albery, W. J., & Knowles, J. R. (1976) *Biochemistry 15*, 5627.
Altman, S. (1989) *Adv. Enzymol. 62*, 1.
Altman, S., & Guerrier-Takada, C. (1986) *Biochemistry 25*, 1205.
Barshop, B. A., Wrenn, R. F., & Frieden, C. (1983) *Anal. Biochem. 130*, 134.
Bevilacqua, P. C., Kierzek, R., Johnson, K. A., & Turner, D. H. (1992) *Science 258*, 1355.
Davanloo, P., Rosenberg, A. H., Dunn, J. J., & Studier, F. W. (1984) *Proc. Natl. Acad. Sci. U.S.A. 81*, 2035.
Dawson, M. C., Elliott, D. C., Elliott, W. H., & Jones, K. M. (1986) in *Data for Biochemical Research*, p 103, Oxford University Press, New York.
Fedor, M. J., & Uhlenbeck, O. C. (1992) *Biochemistry 31*, 12042.
Fersht, A. (1985) in *Enzyme Structure and Mechanism*, p 153, W. H. Freeman and Company, New York.
Fierke, C. A., & Hammes, G. G. (1994) *Methods Enzymol.* (in press).
Fierke, C. A., Johnson, K. A., & Benkovic, S. J. (1987a) *Biochemistry 26*, 4085.
Fierke, C. A., Kuchta, R. D., Johnson, K. A., & Benkovic, S. J. (1987b) *Cold Spring Harbor Symp. Quant. Biol. LII*, 631.
Hammes, G. G. (1982) *Enzymatic Catalysis and Regulation*, p 99, Academic Press, New York.
Hardt, W. D., Schlegl, J., Erdmann, V. A., & Hartmann, R. K. (1993) *Nucleic Acids Res. 21*, 3521.
Herschlag, D. (1992) *Biochemistry 31*, 1386.
Herschlag, D., & Cech, T. R. (1990) *Biochemistry 29*, 10159.
Herschlag, D., & Khosla, M. (1994) *Biochemistry 33*, 5291.
Herschlag, D., Piccirilli, J. A., & Cech, T. R. (1991) *Biochemistry 30*, 4844.
Johnson, K. A. (1986) *Methods Enzymol. 134*, 677.
Johnson, K. A. (1992) in *The Enzymes, Vol. XX*, p 10, Academic Press, Orlando, FL.
Mayer, R. J., Chen, J. T., Taira, K., Fierke, C. A., & Benkovic, S. J. (1986) *Proc. Natl. Acad. Sci. U.S.A. 83*, 7718.
McClain, W. H., Guerrier-Takada, C., & Altman, S. (1987) *Science 238*, 527.
Milligan, J. F., & Uhlenbeck, O. C. (1989) *Methods Enzymol. 180*, 51.
Pace, N. R., & Smith, D. (1990) *J. Biol. Chem. 265*, 3587.
Penefsky, H. S. (1979) *Methods Enzymol. 56*, 527.
Pyle, A. M. (1993) *Science 261*, 709.
Pyle, A. M., & Green, J. B. (1994) *Biochemistry 33*, 2716.
Pyle, A. M., McSwiggen, J. A., & Cech, T. R. (1990) *Proc. Natl. Acad. Sci. U.S.A. 87*, 8187.
Reich, C., Olsen, G. J., Pace, B., & Pace, N. R. (1988) *Science 239*, 178.
Robertson, H. D., Altman, S., & Smith, J. D. (1972) *J. Biol. Chem. 247*, 5243.
Rose, I. A. (1980) *Methods Enzymol. 64*, 47.
Sambrook, J., Fritsch, E. F., & Maniatis, T. (1989) in *Molecular Cloning: A Laboratory Manual*, 2nd ed., pp 6.36 and E.37, Cold Spring Harbor Laboratory Press, Plainview, NY.
Segel, I. W. (1975) in *Enzyme Kinetics: Behavior and Analysis of Rapid Equilibrium and Steady-State Enzyme Systems*, p 506, John Wiley & Sons, Inc., New York.
Silverman, D. N., & Lindskog, S. (1988) *Acc. Chem. Res. 21*, 30.
Smith, D., & Pace, N. R. (1993) *Biochemistry 32*, 5273.
Smith, D., Burgin, A. B., Haas, E. S., & Pace, N. R. (1992) *J. Biol. Chem. 267*, 2429.
Tallsjö, A., & Kirsebom, L. A. (1993) *Nucleic Acids Res. 21*, 51.
Thurlow, D. L., Shilowski, D., & Marsh, T. L. (1991) *Nucleic Acids Res. 19*, 885.
Williams, R. J., & Lansford, E. M. (1967) in *The Encyclopedia of Biochemistry*, p 643, Reinhold Publishing Corporation, New York.
Young, B., Herschlag, D., & Cech, T. R. (1991) *Cell 67*, 1007.
Zaug, A. J., Grosshans, C. A., & Cech, T. R. (1988) *Biochemistry 27*, 8924.